First Libyan international Conference on Engineering Sciences & Applications (FLICESA_LA)
13 – 15 March 2023, Tripoli – Libya

Photon Coincidence Simulation Through Virtual Chaotic Light Source Timestamps

Jamal M. Ehtaiba
Dept. of Electrical Technologies
High Institute of Science and Technology
Misurata, Libya

Ehtaiba_j@yahoo.co.uk

***Abstract*— An ideal single-photon detector can produce one output signal for every single-photon incidence. However, true photodetection systems have time response issues that restrict their detection efficiency and lack photon number counting accuracy. Here, and through simulation, we show that a low time resolution property of a single-photon detector has a remarkable influence on the second coherence function of light photons. We find that photon bunching property pervades source second-order coherence as detector time resolution falls. In the simulation, we use randomly generated timestamps of normal distributions to virtually represent a chaotic light of different mean and variance. In addition, we also present photon decay time and zero arrival delay time second-order coherence computations. This simulation approach has benefits in developing both single-photon sources and single-photon detectors.**

***Keywords*—chaotic light, coincidence, coherence, timestamps, single-photon**

I. INTRODUCTION

Photons emerging from different light sources comparably have different photon statistics that describe the kind of light source, chaotic, coherent, or quantum. The first class has photon statistics of super Poisson distribution with photon number variance larger than the photon number mean. Photons emitted from a chaotic light source are usually referred to as bunched photons [1, 2] and are characterized by more likely queuing closely spaced in time than to queue further apart. All thermal-like sources exhibit the bunching property in photon statistics. Conversely, a quantum light source (also called non-classical light source) exhibits antibunching property of photon statistics (sub Poissonian) where photons propagate more likely far apart in time than close together [3, 4]. On the other hand, a coherent light source is the source that generates light with Poissonian photon number statistics that are neither bunched nor antibunched [5, 6]. The focus will be on the bunched chaotic photons throughout our discussion in this paper.

Measuring the antibunching degree of photons emitted from a light source can be performed through observing the second order correlation function (sometimes referred to as second order coherence) $g^{(2)}(\tau)$, of the light source. A Hanbury Brown, and Twiss (HBT) interferometer with two independent photodetectors, each attached to a particular channel is typically used to measure $g^{(2)}(\tau)$ [7], see Fig. 1.

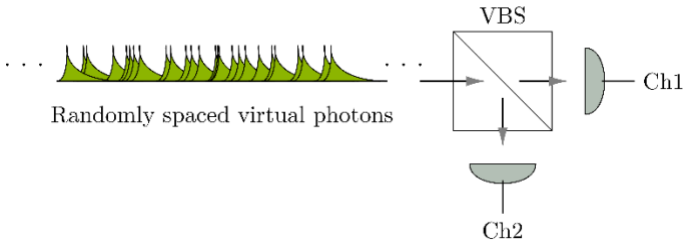

Fig. 1. HBT interferometer, schematic diagram with an input virtual photon stream of a normal random time spacing. The notion VBS is an abbreviation for virtual beam splitter.

The degree of second-order correlation function is given as in (1) [8], Where I represents average intensity of the incident field on the 50:50 beam splitter (shown as VBS in Fig. 1), and τ is the arrival delay time between the two fields at the photodetectors' active areas.

$$g^{(2)}(\tau) = \frac{\langle \bar{I}(t)\bar{I}(t+\tau)\rangle}{\bar{I}^{2}} \qquad (1)$$

Equation (1) shows that the second-order coherence is an intensity-intensity correlation function normalized to the average intensity value. In our simulation work, the correlation is carried out through histograms built of a large number of virtual timestamps recorded by the two HBT channels. Also, from (1),

we can easily notice that $g^{(2)}(0)$ for a chaotic light source is always greater than or equal to one as the denominator I^2 (equivalent to $\langle I(t)\rangle^2$) is always less than or equal to the numerator $\langle I(t)^2\rangle$ [8].

Getting information about photon emission statistics through the second coherence function is extremely important particularly when charactering single-photon sources built from quantum emitters e.g., quantum dots [9], vacancy centers [10], and nanoparticles [11]. For instance, a value of $g^{(2)}(0) > 1$ is an indication to bunched photons, a value of $g^{(2)}(0) = 1$ refers to coherent (laser) light, and a value of $0 \leq g^{(2)}(0) < 1$ reveals antibunched photons. However, photodetector response time plays a key role in determining the quality of the single-photon emitter, because shorter response time allows photon counting coincidences more precisely at real measurements of $g^{(2)}(\tau)$ [.

Since ideal single-photon detectors with zero timing latency, timing jitter, and dead time do not exist, accurate measurement of $g^{(2)}(\tau)$ would be elusive, especially when the detection system has no photon number resolving capability. For instance, a zero-photon coincidence might not be registered by an HBT interferometer if its detectors' time resolution is larger than the timestamp gap between two successive incident photons [12]. In the coming sections, we denote the time resolution as coincidence time window (cw).

Here, we simulate the influence of changing coincidence time window on the second-order coherence of a virtual and randomly generated photon timestamps. To ensure bunching property of generated virtual photons, we purposely made the variance of each timestamp set larger than the mean in a normal distribution.

II. SIMULATION STEPS

A. Prepare timestamps

To simulate thermal source photons hit detectors D1 and D2 of the virtual HBT interferometer shown in Fig. 1, we first use MATLAB software to randomly generate virtual timestamps of some mean and variance from a normal probability distribution. Also, we ensure the functionality of the simulation program by creating three sets of timestamps (μ_1, ν_1), (μ_2, ν_2), and (μ_3, ν_3), where μ_i and ν_i are the mean and variance for each timestamps set. That is to say, three thermal light sources of similar photon statistics but differ in the mean and variance. In the simulation, we make $\mu_3 > \mu_2 > \mu_1$, $\nu_1 > \mu_1$, $\nu_2 > \mu_2$, and $\nu_3 > \mu_3$. The length of each set is 1000,000 (one million) timestamps. Fig. 2 shows a time slot of set 1 timestamps, labeled source. Of course, the units of the generated timestamps are generally arbitrary time units, but here we assume seconds as standard time units for our data.

B. Splitting timestamps

Before the photon beam (timestamps) reach the HBT interferometer detectors, they first hit the beam splitter (VBS in Fig. 1) which guides every single photon either to detector D1 or to detector D2 based on a uniform random control value between 0.0 and 1.0. In the event that the control random value is less than or equal to 0.5, the timestamp is registered in channel 1 (Ch1 in Fig. 1) through detector D1, and it is registered in channel 2 (Ch2 in Fig. 1) through detector D2 otherwise. This process repeats for the whole virtual photon time sequence hits the virtual beam splitter.

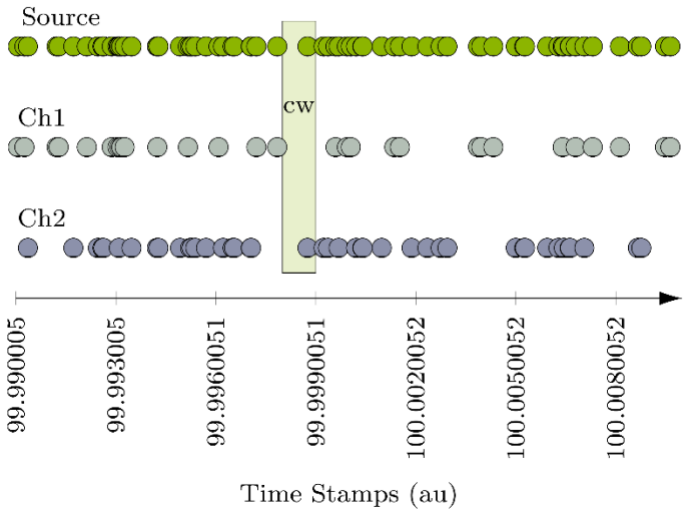

Fig. 2 Virtual photon timestamps. Top circles line labeled source is set 1 data before hitting the VBS. Middle line circles labeled Ch1 represents photon timestamps guided to channel 1 of the HBT interferometer. Bottom circles line represents photon timestamps guided to channel 2. The cw rectangle represents detection system coincidence time window.

Fig. 3. shows decay times for the three timestamp sets. The decayed data, and the fit lines, built through histograms of differences in arrival times of virtual photons at the two detectors. The decay times obtained for each of the data are shown on the figure. The decay times are in microseconds based on our assumption that the created data sets are in seconds. One can easily notice that decay time increases as the timestamp random data mean increases since μ_3 is the largest. We didn't take any steps to check the influence of changing the coincidence time window on decay times considering a perfect recording for every arrived photon.

C. Correlating timestamps

In this section we discuss the computation routine for the second-order coherence function. Based on the timestamps data recorded in channels 1 and 2, we build histograms from each channel record and sweep a time window of limited width over the whole-time range of the histograms. The width of the time

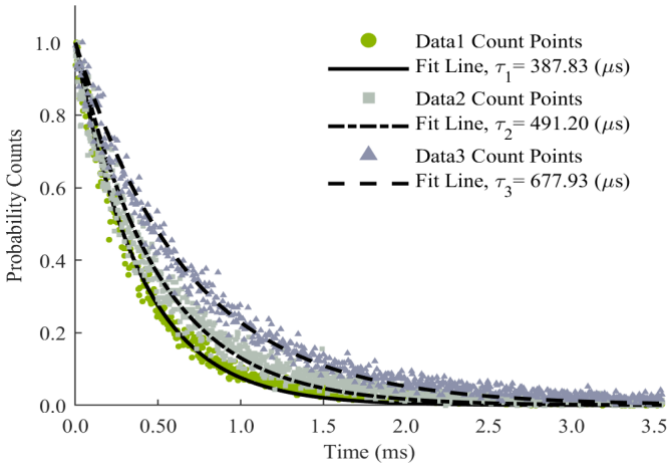

Fig. 3 Decay time for the three chaotic light sources, computed through differences in arrival times at detectors 1 and 2 of the HBT interferometer. Indicated values for the decay times are based on the assumption that the source photon timestamps are given in seconds.

Window is determined by the decay time of the timestamps data under simulation (τ_2 in this case). The smallest coincidence time window used in the simulation is ~ 98 µs which is only 20% of the decay time. In like manner, the largest coincidence time window taken in the simulation is ~ 0.49 s which is $1000.1\tau_2$. The histogram values of both channels data are then cross correlated to find $g^{(2)}(\tau)$. Eventually, the average value of $g^{(2)}(\tau)$ is taken for over 50 repetition times of correlation process.

III. SIMULATION RESULTS AND DISCUSSION

Fig. 4 shows the simulation result for the second coherence function against delay time for various coincidence time window values. We see that as the coincidence time window width decreases, $g^{(2)}(0)$ goes down and the photons exhibit less bunching property, the photon statistics come closer to the coherent photon state. In contrast, as the coincidence time window increases in width, the bunching property of the photons source becomes more clearer and $g^{(2)}(0)$ reaches maximum value, 2. In practice, tuning the detection system to a high time resolution may not be available leading to inaccurate reading for $g^{(2)}(0)$. So, knowledge about the decay time of the photons source helps choosing the proper detector to characterize the source.

Fig. 5 is a plot of $g^{(2)}(0)$ against the coincidence time window for the three data sets. The figure illustrates the rapid transition of $g^{(2)}(0)$ from its lowest values at high time resolution of the detector towards the maximum as the detector loses resolution.

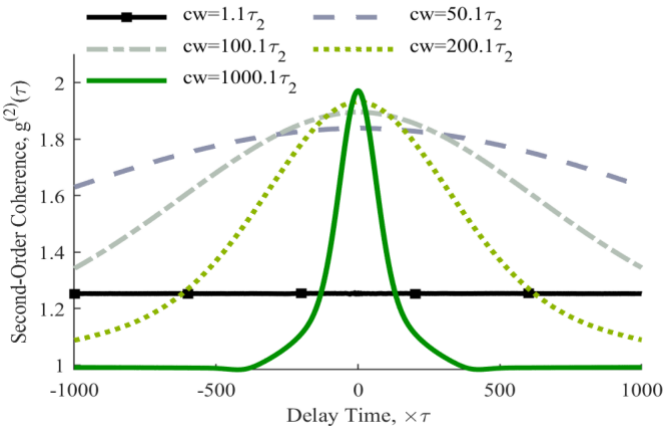

Fig. 4. Second-order coherence versus coincidence time window. All lines represent source s2. The other two sources have similar behavior.

IV. CONCLUSION

In conclusion, we simulated the second-order coherence of bunched photons through randomly generated timestamps of different decay times. We found that bunched photon statistics property of a light source dominates as the detection system resolution time is limited compared to the photons decay time. Conversely, a bunched photons source exhibits less bunching property with high-time resolution detectors. The simulation results show considerable benefits and can be useful for

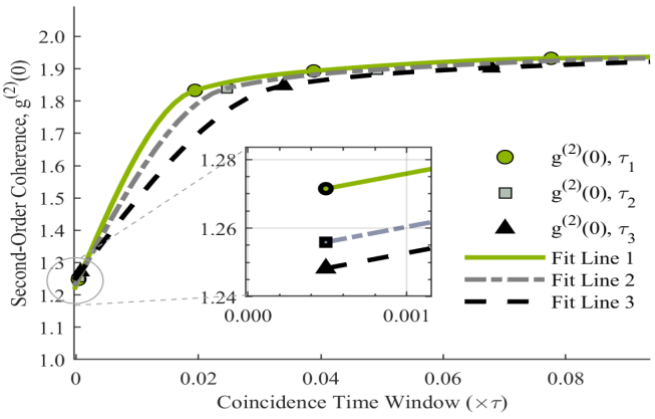

measuring photon emitters', particularly single-photon sources, second-order coherence function.

Fig. 5. $g^{(2)}(0)$ as a function of the coincidence time window.

V. REFERENCES

[1] B. L. Morgan and L. Mandel, "Measurement of Photon Bunching in a Thermal Light Beam," *Physical Review Letters,* vol. 6, no. 22, p. 1012, 1966.

[2] S. Meuret and et al., "Photon Bunching in Cathodoluminescence," *Physical review letters,* vol. 114, no. 19, p. 197401, 2015.

[3] H. J. Kimble, M. Dagenais and L. Mandel, "Photon antibunching in resonance fluorescence," Physical Review Letters, vol. 39, no. 11, p. 691, 1977.

[4] L. Fleury, J. -M. Segura, G. Zumofen, B. Hecht and U. P. Wild, "Nonclassical photon statistics in single-molecule fluorescence at room temperature," Physical review letters, vol. 84, no. 6, p. 1148, 2000.

[5] W. Choi and et al., "Observation of sub-Poisson photon statistics in the cavity-QED microlaser," Physical review letters, vol. 96, no. 9, p. 093603, 2006.

[6] L. C. Phillips and et al., "Photon Statistics of Filtered Resonance Fluorescence," Physical review letters, vol. 125, no. 4, p. 043603, 2020.

[7] H. R. Brown and R. Q. Twiss, "Correlation between photons in two coherent beams of light," Nature, vol. 177, no. 4497, pp. 27-29, 1956.

[8] R. Loudon, The quantum theory of light, OUP Oxford, 2000.

[9] H. Huiying and et al., "Bright Single Photon Emission from Quantum Dots Embedded in a Broadband Planar Optical Antenna," Advanced optical materials, vol. 9, no. 7, p. 2001490, 2021.

[10] H. Siampour and et al., "Ultrabright single-photon emission from germanium-vacancy zero-phonon lines: deterministic emitter-waveguide interfacing at plasmonic hot spots.," Nanophotonics, vol. 9, no. 4, pp. 953-962, 2020.

[11] V. Salakhutdinov and et al., "Single photons emitted by nano-crystals optically trapped in a deep parabolic," Physical Review Letters, vol. 124, no. 1, p. 0136907, 2020.

[12] J. S. Lundeen and et al, "Tomography of quantum detectors," Nature Physics, vol. 5, no. 1, pp. 27-30, 2009.

[13] P. R. Tapster and J. G. Rarity, "Photon statistics of pulsed parametric light," Journal of Modern Optics, vol. 45, no. 3, pp. 595-604, 1998.

[14] P. Kochan and H. J. Garmichael, "Photon-statistics dependence of single-atom absorption," Physical Review A, vol. 50, no. 2, p. 1700, 1994.

[15] Y. Guo and et al., "Photon statistics and bunching of a chaotic semiconductor laser," Optics express, vol. 26, no. 5, pp. 5991-6000, 2018.